An *in vitro* setup to test the relevance and the accuracy of low-order vocal folds models

Nicolas Ruty, Xavier Pelorson, and Annemie Van Hirtum
Institut de la Communication Parlée, UMR5009 CNRS/INPG/Université Stendhal, 46 Avenue Félix Viallet, 38031 Grenoble Cedex 01, France

Ines Lopez-Arteaga
Department of Mechanical Engineering, Dynamics and Control, Eindhoven University of Technology, P.O. Box, 513, WH-1.129, 5600 MB Eindhoven, The Netherlands

Avraham Hirschberg
Department of Applied Physics, Gas Dynamics and Aero-acoustics, Eindhoven University of Technology, P.O. Box 513, CC 2.24, 5600 MB Eindhoven, The Netherlands

(Received 28 February 2006; revised 30 August 2006; accepted 7 October 2006)

An experimental setup and human vocal folds replica able to produce self-sustained oscillations are presented. The aim of the setup is to assess the relevance and the accuracy of theoretical vocal folds models. The applied reduced mechanical models are a variation of the classical two-mass model, and a simplification inspired on the delayed mass model for which the coupling between the masses is expressed as a fixed time delay. The airflow is described as a laminar flow with flow separation. The influence of a downstream resonator is taken into account. The oscillation pressure threshold and fundamental frequency are predicted by applying a stability analysis to the mechanical models. The measured frequency response of the mechanical replica together with the initial (rest) area allows us to determine the model parameters (spring stiffness, damping, geometry, masses). Validation of theoretical model predictions to experimental data shows the relevance of low-order models in gaining a qualitative understanding of phonation. However, quantitative discrepancies remain large due to an inaccurate estimation of the model parameters and the crudeness in either flow or mechanical model description. As an illustration it is shown that significant improvements can be made by accounting for viscous flow effects.
[DOI: 10.1121/1.2384846]

PACS number(s): 43.70.Jt, 43.70.Bk [AL] Pages: 479–490

I. INTRODUCTION

Schematically, phonation can be understood as the result of a complex interaction between respiratory airflow and soft tissues. Under certain circumstances, the ongoing fluid/structure interaction can result in self-oscillation of the vocal folds. Vocal fold auto-oscillation produces the main sound source for the vocal tract during the production of voiced sounds.

Physical modeling of this process is obviously needed for many practical applications, especially in the field of voice synthesis and pathology. Although some important advances have been made in the field, full numerical models of phonation, based on finite element models for the tissues, for example (Hunter *et al.*, 2004; Vampola *et al.*, 2005), are still underused. This can be understood firstly because of the numerical complexity of such an approach, which implies, in particular, hours of computation time. Secondly, it must be noted that an accurate description of many physical effects such as the collision of the vocal folds, the way to account for unsteady boundary conditions, or the presence of turbulence in the flow, just to name a few, are far beyond the capabilities of most common numerical software.

For these reasons, low-order models, often called distributed (or lumped) models, are still very popular because of their simplicity. Such models are indeed often used for speech synthesis purposes (Flanagan *et al.*, 1975; Story and Titze, 1995; Kob, 2002), but low-order models have also been used in speech pathology studies (Wong *et al.*, 1991; Herzel *et al.*, 1994; Lous *et al.*, 1998). One major concern about these low-order models is the crudeness of the physics used in the models. This includes the fluid mechanics of the airflow through and past the glottis, the biomechanics of the vocal fold tissues, and the acoustics of the vocal tract as well as the interactions between these physical processes.

Concerning the description of the airflow, many attempts have been performed in order to test theories of varying complexity. While some attempts to measure pressure and flow *in vivo*, i.e., on human speakers, have been performed (Van den Berg *et al.*, 1957; Cranen, 1987) most experiments deal with *in vitro* setups based on a mechanical replica of the larynx. Flow measurements on a rigid nonoscillating replica of the vocal folds have been performed by van den Berg *et al.* (1957), Scherer *et al.* (1983, 2001), Pelorson *et al.* (1995), and Hofmans *et al.* (2003). More complex, and realistic, flow conditions were recently obtained using oscillating replicas of the larynx (Titze *et al.*, 1995; Barney *et al.*, 1999; Deverge *et al.*, 2003; Mantha *et al.*, 2005; Thomson *et al.*, 2005). In particular, self-oscillating replicas are of great interest because they allow us to test not only the flow description, but

also the interaction with a mechanical (eventually deformable) structure and with an acoustical resonator. This type of deformable replica is also used to study lip behavior during buzzing in musical acoustics (Gilbert *et al.*, 1998; Cullen *et al.*, 2000; Vilain *et al.*, 2003).

Another major concern with low-order models deals with the relevance of the model itself with respect to the vocal fold physiology. While some parameters of the models, like the subglottal pressure or the geometry of the glottis, can be directly compared to observations performed on humans, others, like springs or dampers in a two-mass model such as Ishizaka and Flanagan (1972), have no direct equivalent in real life. The existence and the way to derive a relationship between these parameters and human physiology is therefore a crucial problem. Some important studies (Svec *et al.*, 2000; Berry and Titze, 1996; Berry *et al.*, 1994; Kaneko *et al.*, 1983; De Vries, 1999; Childers and Wong, 1994) have been performed using either *in vivo* measurements or numerical simulations of some mechanical properties of human vocal folds. While these data are helpful to derive the mechanical parameters of low-order models, they do not allow for testing the models themselves.

In this paper we present an experimental setup designed to test low-order models of the vocal folds including the mechanics, the fluid mechanics, the acoustics, and their interactions. This setup relies on a self-oscillating replica consisting of a pair of thin latex tubes filled with water. Although it behaves in a comparable way, this replica is not intended to be viewed as a "real" larynx but rather as a test for the relevance of the theoretical models. Compared with "real life" experiments, this setup has the advantage of easy control and quantitative access to most important fluid mechanical and mechanical parameters. In particular, thanks to an optical device, the mechanical response of the replica can be measured. Using the same device, the vibration of the replica can be quantitatively observed. Two low-order models of the vocal folds are tested. First, a modification of the original two-mass vocal fold model of Ishizaka and Flanagan is presented. Second, a further simplification exploiting only one single degree of freedom to describe the tissue mechanics is considered. Next, stability analysis is applied in order to evaluate the performance of the theoretical predictions against the experimental data.

II. MODELS UNDER TEST

Two theoretical models of the complex phonatory apparatus are described. These models are severe simplifications of the fluid structure interactions appearing during human voiced sound production. The interaction between airflow and mechanical models of the vocal folds is described in Sec. II A. The two mechanical models are detailed in Sec. II B. The acoustic interaction between the voiced sound source and the vocal tract, using a linear acoustic approximation, is described in Sec. II C.

A. Flow model

The geometry of the glottal channel is schematically depicted in Fig. 1. For the sake of simplicity, the simplest approximation for the glottal flow has been chosen. This description relies on the assumption of a quasi-steady inviscid and incompressible flow within the glottis. Further, the subglottal pressure P_{sub} is assumed to be constant and independent from the other characteristic values of the system. Lastly, when the glottis forms a diverging channel, the flow is assumed to separate at a position determined by the following *ad hoc* criterion $\text{As}(t)=1.2^{*}\min(A(x,t))$ with $A(x,t)$ being the glottal cross-sectional area and $\text{As}(t)$ the glottal area at the separation point. Using these assumptions one can predict the instantaneous pressure within the glottis, $P(x,t)$, as

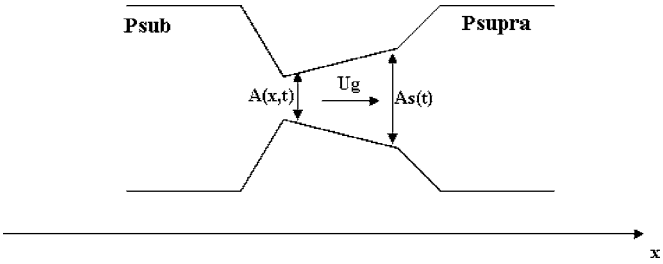

FIG. 1. Geometry used for the fluid mechanical description. Psub is the subglottal pressure, Psupra is the supraglottal pressure, $A(x,t)$ is the transversal area of the glottis along the X coordinate, U_g is the volume flow, and $\text{As}(t)$ denoted the transversal area of the glottis at separation point.

$$P_{\text{sub}} - P(x,t) = \frac{1}{2}\rho U_g^2\left(\frac{1}{A^2(x,t)}\right), \quad \text{if } x < x_s,$$

$$P(x,t) = P_{\text{supra}}, \quad \text{if } x > x_s, \tag{1}$$

where ρ indicates the constant air density, U_g is the volume flow velocity, and P_{supra} is the supraglottal pressure.

Neglecting the effects of wall vibrations, the volume flow velocity, U_g, is a constant that can be predicted from the overall pressure drop at the glottis:

$$U_g = \sqrt{\frac{2(P_{\text{sub}} - P_{\text{supra}})}{\rho(1/A_s^2)}}. \tag{2}$$

Equation (2) can be simplified as

$$U_g = A_s\sqrt{\frac{2(P_{\text{sub}} - P_{\text{supra}})}{\rho}}. \tag{3}$$

Combining Eqs. (3) and (1) the pressure distribution is written as

$$P(x,t) = P_{\text{sub}} - (P_{\text{sub}} - P_{\text{supra}})\left(\frac{A_s^2}{A^2(x,t)}\right), \quad \text{if } x < x_s,$$

$$P(x,t) = P_{\text{supra}}, \quad \text{if } x > x_s. \tag{4}$$

B. Mechanical principles

The mechanical properties of the vocal folds are represented by the distributed model depicted in Fig. 2. It is assumed that the glottis has a constant width, L_g. Applying the second principle of dynamics to these models, the following equations are obtained:

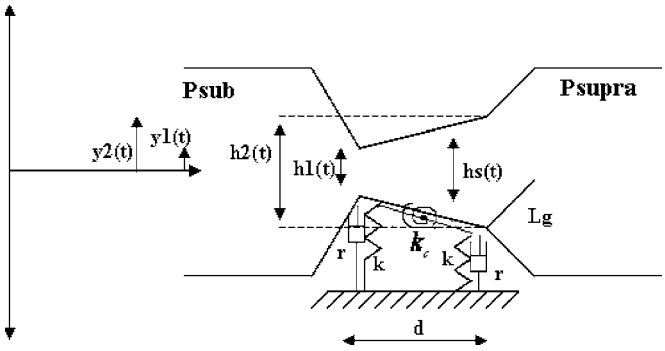

FIG. 2. Two mass model of the vocal folds. y1(t) and y2(t) are the movements on the *Y* coordinate, h1(t) and h2(t) are the apertures of the glottis, hs(*t*) is the aperture of the glottis at separation point, Lg denotes the vocal fold width, d is the length of the vocal folds, k and k_c denote the spring stiffness, and *r* is the damping.

$$\frac{m}{2}\frac{\partial^2 y_1(t)}{\partial t^2} = -k(y_1(t)-y_{10}) - k_c(y_1(t)-y_{10}-y_2(t)+y_{20}) - r\frac{\partial y_1(t)}{\partial t} + F_1(P_{\text{sub}},P_{\text{supra}},H_1,H_2), \tag{5}$$

$$\frac{m}{2}\frac{\partial^2 y_2(t)}{\partial t} = -k(y_2(t)-y_{20}) - k_c(y_2(t)-y_{20}-y_1(t)+y_{10}) - r\frac{\partial y_2(t)}{\partial t} + F_2(P_{\text{sub}},P_{\text{supra}},H_1,H_2), \tag{6}$$

where m is the effective vibrating mass of a vocal fold, k and k_c indicate the spring stiffnesses, r is the damping, d is the length of the glottis, $y_1(t)$ and $y_2(t)$ denote the positions of the two masses, y_{10} and y_{20} are the rest positions of the two masses, and F_1 and F_2 are the pressure forces along the y axis.

The pressure force distribution is derived from the description of Lous *et al.* (1998). We assume a symmetrical movement of the two vocal folds. Consequently, $H(t)=2y(t)$ and Eq. 6 become

$$\frac{\partial^2 H_1(t)}{\partial t^2} = -\frac{2k}{m}(H_1(t)-H_{10}) - \frac{2k_c}{m}(H_1(t)-H_{10}-H_2(t)+H_{20}) - \frac{2r}{m}\frac{\partial H_1(t)}{\partial t} + \frac{4}{m}F_1(P_{\text{sub}},P_{\text{supra}},H_1,H_2),$$

$$\frac{\partial^2 H_2(t)}{\partial t} = -\frac{2k}{m}(H_2(t)-H_{20}) - \frac{2k_c}{m}(H_2(t)-H_{20}-H_1(t)+H_{10}) - \frac{2r}{m}\frac{\partial H_2(t)}{\partial t} + \frac{4}{m}F_2(P_{\text{sub}},P_{\text{supra}},H_1,H_2). \tag{7}$$

This formulation can be simplified if the time delay between the movements of the two masses is assumed to be constant in time. This hypothesis is proposed by Avanzini *et al.* (2001) and as a result Eq. (7) can be simplified since only the movement of the first mass needs to be described while the movement of the second mass is supposed to follow the first one with a fixed time delay t_0. In other words, the coupling between the two masses is now described by the parameter t_0 accounting for the fixed time delay instead of the coupling spring k_c. Consequently, only a single mechanical degree of freedom remains:

$$\frac{\partial^2 H_1(t)}{\partial t^2} = -\frac{2k}{m}(H_1(t)-H_{10}) - \frac{2r}{m}\frac{\partial H_1(t)}{\partial t} + \frac{4}{m}F_1(P_{\text{sub}},P_{\text{supra}},H_1(t),H_1(t-t_0)),$$

$$H_2(t) = H_1(t-t_0). \tag{8}$$

In the following we will refer to this simple description as the delayed mass model. This approach is comparable to the model proposed by Titze (1988) and more recently by Drioli (2005). Note that if the delay t_0 equals zero, the model reduces then to a one-mass model, such as the one described by Flanagan and Landgraf (1968) and by Cullen *et al.* (2000).

A special case occurs when the vocal folds are colliding. Following Ishizaka and Flanagan (1972), this phenomenon is simply modeled as a discrete change in the spring stiffnesses and dampings:

$$k_{1e} = 4*k_1, \quad r_{1e} = r_1 + 2*\sqrt{k_{1e}*m/2} \quad \text{if } H_1 < 0,$$

$$k_{2e} = 4*k_2, \quad r_{2e} = r_2 + 2*\sqrt{k_{2e}*m/2} \quad \text{if } H_2 < 0, \tag{9}$$

where k_{1e}, k_{2e} denote the modified spring stiffness and r_{1e}, r_{2e} are the modified damping.

C. Acoustical description

Acoustical coupling with the vocal tract is only expected to be significant when the fundamental frequency of the vocal folds oscillation becomes close to a formant frequency (typically the first formant for normal speech), as described by Rothenberg (1980). Therefore, for the sake of simplicity, the acoustics of the downstream resonator is assimilated to a single degree of freedom system described by the following equation,

$$\frac{\partial^2 \psi(t)}{\partial t^2} + \frac{\omega_A}{Q_A}\frac{\partial \psi(t)}{\partial t} + \omega_A^2 \psi(t) = \frac{Z_A \omega_A}{Q_A} u, \tag{10}$$

where $\partial\psi(t)/\partial t = p$, with p the acoustic pressure at the entrance of the resonator, ω_A is a resonance pulsation of the resonator, Q_A is the quality factor of this resonance, Z_A is the peak value of impedance at resonance ω_A, and u is the acoustic airflow velocity.

In other words, this description is equivalent to the classical linear theory of the vocal tract (Flanagan, 1972), but accounts only for the first acoustical resonance of the downstream resonator. The vocal tract is simply described by the impedance of an unflanged pipe radiating in free space (Pierce, 1991), but only the first acoustical resonance of the downstream resonator is taken into account.

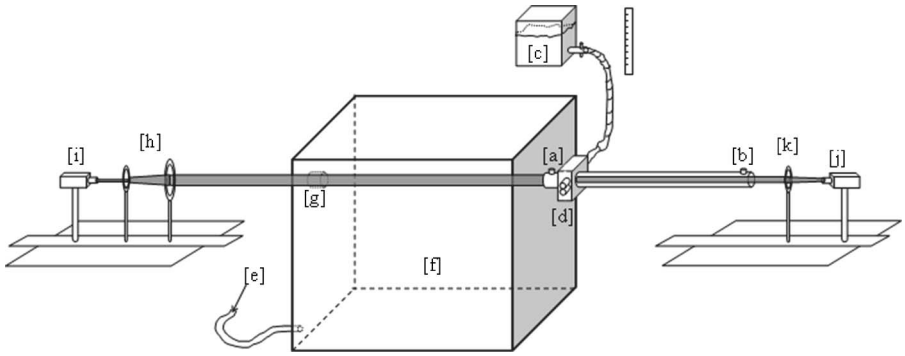

FIG. 3. Experimental setup, replicating the human phonatory apparatus. (a), (b) Pressure transducer plug. (c) Water tank supplying the fixed internal pressure inside the latex tubes of the vocal fold replica. (d) Deformable replica of the vocal folds. (e) Air supply. (f), Pressure tank, walls covered with absorbing foam. (g) Transparency window. (h), (k) Optical lenses. (i) Laser diode. (j) Photodiode.

III. EXPERIMENTAL SETUP

The theoretical models described in the previous section need to be validated. *In vivo* measurements have the advantage of being performed on real human tissues, but the lack of control and reproducibility is a severe drawback, which can harm the validation robustness. For this reason, in the literature, several *in vitro* experimental studies on relevant mechanical replicas have been performed in order to validate different aspects of the interacting theoretical models (fluid mechanical, mechanical, or acoustical). Steady rigid replicas have been used to validate the theoretical description of quasi-steady flow (e.g., Van den Berg *et al.*, 1957; Scherer *et al.*, 1983; Gauffin *et al.*, 1983; Gauffin and Liljencrants, 1988; Scherer and Guo, 1990; Scherer *et al.*, 2001; Pelorson *et al.*, 1994, 1995). More recently, the influence of wall displacement and structure deformation on the airflow have been considered by using respectively rigid mobile larynx replicas (Kiritani *et al.*, 1987; Barney *et al.*, 1999; Alipour and Scherer, 2001; Deverge *et al.*, 2003) and deformable larynx replicas (Titze *et al.*, 1995; Chan *et al.*, 1997; Thomson *et al.*, 2005). The presented setup follows the same approach. In particular, the various interactions between acoustics, mechanics, and fluid mechanics are investigated.

A. Description

The replica of the larynx is mounted in a suitable experimental setup illustrated in Fig. 3. The lungs are represented by a pressure reservoir of 0.75 m^3 fed by a compressor. The walls of the reservoir have been covered with absorbing foam in order to reduce acoustical resonances of the reservoir. The reservoir pressure is controlled by means of a Norgren pressure regulator type 11-818-987 and could be varied from a few Pa up to 3000 Pa.

A vocal fold replica, depicted in Figs. 4 and 5, is connected to the reservoir. This replica, upscaled by a factor 3 compared with real vocal folds, consists of two metal half cylinders of 12.5-mm diameter, covered with latex tubes (Piercan Ltd.) of 11-mm diameter (±0.1 mm) and 0.2 mm thickness (±10%). The two cylinders are filled with water under pressure. The water pressure, henceforth denoted the internal pressure Pc, is controlled by means of a water column. Changing the height of the column allows us to impose an internal pressure Pc up to 10 000 Pa. The value of the internal pressure Pc has an influence on the replica's mechanical characteristics, but also on the initial replica opening. Typically, for low values of Pc (e.g., 2500 Pa), the initial replica aperture is of the order of 2 mm and the latex tension is low, while for larger values of Pc (of the order of 6000 Pa), the two latex tubes are in contact, and the tension increases. The acoustics of the vocal tract can be simulated using an acoustic resonator connected downstream to the replica. For this study, two different tubes of uniform circular section (diameter 25 mm) were used. Their lengths are respectively 500 and 250 mm.

This experimental setup has been carefully designed in order to match as much as possible the order of magnitudes relevant for physical quantities during speech production. The relevance of the experimental design can be assessed using quantitative considerations based on a dimensionless analysis. The Reynolds number $\mathrm{Re}=\rho V_g h_g/\mu$, where ρ is the air density, V_g is the mean flow velocity, h_g is the replica aperture, and μ is the dynamic viscosity coefficient of air, can be used as a measure of the importance of viscosity relative to inertial forces in the flow. The Strouhal number $S_r=fd/V_g$, where f is the oscillation fundamental frequency and d is the longitudinal length of the replica, is a measure

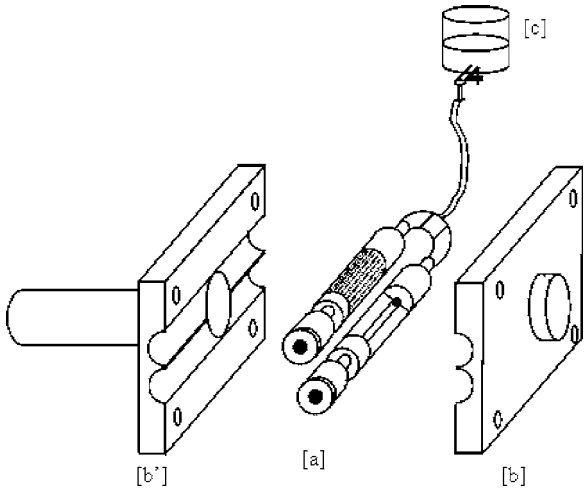

FIG. 4. Deformable replica of the vocal folds (Vilain *et al.*, 2003). Tension is controlled by the water pressure. (a) Brass half-cylinder, covered by latex tubes, and filled with water. (b), (b) Steel support.

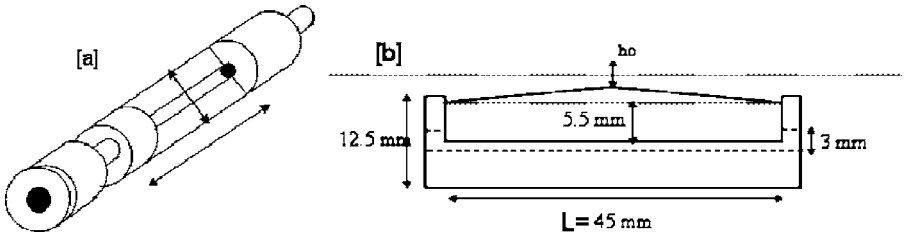

FIG. 5. Details of a vocal fold replica. (a) Isometric view of a half cylinder covered by latex tube. (b) Frontal view used to estimate the water volume filing the latex tube.

for the importance of inertia in the flow compared to convection. The Mach number $\mathrm{Ma}=V_g/c_0$, where c_0 is the speed of sound, provides a measure for the importance of compressibility effects. Other parameters, such as the geometrical aspect or the acoustical resonance frequency, are also to be considered. The correspondence between the replica and *in vivo* data is summarized in Table I.

The experimental setup allows two types of dynamical measurements: pressure and geometry. Pressure measurements are performed by means of two Kulite pressure sensors XCS-0.93-0.35-Bar-G, supplied by a Labor-Netzgerat power supply EA-3005S. They are calibrated against a manometer with typical accuracy of ∓ 5 Pa. The pressure sensors were respectively located just upstream from the vocal fold replica and at the end of the resonator tube. The geometrical measurements are performed using an optical device composed of a laser diode, supplied by a P. Fontaine Dc amplifier FTN2515. The laser beam width is increased by two convergent lenses (L1, $f=50$ mm; L2, $f=100$ mm) and passes through the air reservoir thanks to a small Plexiglas window and proceeds through the vocal folds replica. The transmitted laser beam intensity is therefore modulated by the movement of the vocal folds replica. These variations in light intensity are measured using a photo sensor BPW34, supplied by a Solartron Dc Power Supply. The optical system is calibrated by rectangular apertures with known dimensions of 0.01 mm precision.

Electrical signals are amplified and conditioned using a preamplifier/conditioning board (National Instruments SXCI-1121) connected to a PC through a National Instruments BNC-2080 Card and a National Instruments PCI-MIO-16XE acquisition card. The acquired data are processed using Labview7 software (National Instruments).

B. Determination of the model parameters

In order to compare the theoretical model predictions with the experimental data, the relationship between empirical parameters and model parameters must be known. While this relationship can be derived directly for some parameters, like the geometrical dimensions of the glottis (L_g and d), others need to be estimated.

The mass, m, used to describe the mechanics of the theoretical models is estimated by the quantity of water inside the latex tube covering the metal half-cylinder depicted in Fig. 5. The mass is estimated as

$$m_{cv} = \rho_e L \frac{\pi d_l^2}{8} \tag{11}$$

where ρ_e is the density of water, L is the replica width, and d_l is the diameter of the latex tube (11 mm). Considering the dimensions of the replica, the estimated mass of water inside one latex tube for $dl=11$ mm is $m_{cv}=2.29g$. This mass is in fact the maximum mass able to oscillate.

The spring stiffness and damping are estimated thanks to the direct measurement of the mechanical response of the replica. The experimental procedure follows the one used by Gilbert *et al.* (1998) on artificial lips. A pressure driver unit (ERS TU-100) terminated by a cone is used as an acoustical excitation, as shown in Fig. 6. For each acoustical excitation frequency the replica response is obtained by measuring the variation of the distance between the two latex tubes. The

TABLE I. Comparative table: physiological characteristics of for male adult voice [typical "*in vivo*" data obtained from Hollien and Moore (1960), Hirano *et al.* (1983), Saito *et al.* (1981), Mc Glone and Shipp (1971), and Fitch and HolBrook (1970), and Baken, (1987)] and geometrical, dynamical, and acoustical characteristics of the replica.

	Human voice	Replica
Scale	1	3
Aspect ratio, Lg/hg, mean value	20	20
Aspect ratio, Lg/d, mean value	3.3	2.5
Operating pressure, range of values	300–1000 Pa	200–1000 Pa
Frequency of oscillations F0, range of values	80–200 Hz	110–170 Hz
Reynolds number, Re, range of values	700–1300	800–2500
Strouhal number, Sr, mean value	0.01–0.02	0.03–0.05
March number, Ma, range of values	0.06–0.12	0.05–0.12
First acoustical resonance	300–1000 Hz (range of values)	170 Hz (500 mm) 340 Hz (25 mm) (discrete values for each downstream resonator)

Estimated from subglottal pressure and aspect ratio.

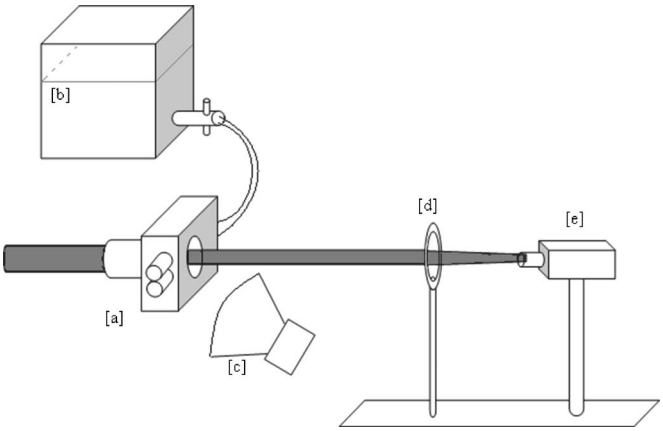

FIG. 6. Experimental setup to measure the mechanical response. (a) Deformable replica of the vocal folds. (b) Water reservoir. (c) Loud speaker, producing the acoustical excitation. (d) Optical lens. (e) Photo diode.

response of the replica is then plotted against the excitation frequency (between 100 and 400 Hz in steps of 1 Hz). This procedure is repeated for each internal pressure Pc between 500 and 6500 Pa in steps of 500 Pa.

A typical example of mechanical response of the replica is depicted in Fig. 7. Note that the retrieved response is quite similar to the mechanical responses observed by Svec *et al.* (2000) on *in vivo* human vocal folds.

From the measured mechanical responses, the resonance frequencies, ω, and associated quality factors, Q, can be easily extracted. The obtained parameters can be related to the natural resonance behavior of the theoretical model of the vocal folds and so to the spring stiffness and damping:

$$\omega_0 = \sqrt{\frac{2k}{m}}, \quad Q_0 = \frac{m\omega_0}{2r}, \tag{12}$$

where ω_0 is the resonance pulsation, Q_0 is the quality factor of this resonance, k is the spring stiffness, $m=m_{cv}/2$, is the

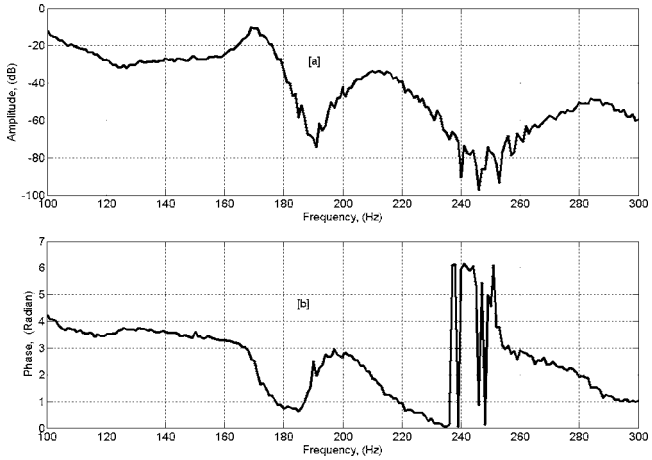

FIG. 7. Mechanical response of the vocal fold replica, internal pressure 2500 Pa. (a) Amplitude of the mechanical response. (b) Phase of the mechanical response.

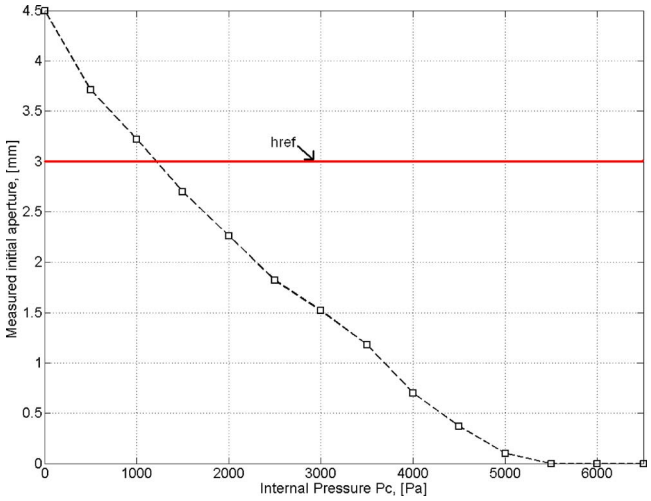

FIG. 8. Measured initial aperture of the vocal fold replica plotted as a function of the internal pressure Pc, varying between 0 and 6500 Pa.

effective mass of a vocal fold, and r is the damping. The coupling spring stiffness k_c is imposed as $k/2$, as described by Lous *et al.* (1998).

When large values of the internal pressure Pc (>5000 Pa) are involved, the frequency response cannot be measured using the above procedure since the two latex tubes are in contact (Fig. 8). For these values of Pc, one of the two latex tubes is removed and the mechanical response of a single tube is measured. The measured response in this case is obviously a very crude approximation since it does not account for the nonlinearity introduced by the contact between the two latex tubes.

IV. RESULTS AND DISCUSSION

In this section, we will detail the comparison between the predictions of the theoretical models and experimental data with respect to two quantitative phonation parameters: the on-set and off-set pressure of oscillation and the fundamental frequency. The measurements are discussed in Sec. IV A and the simulations in Sec. IV B. The comparison between experimental and theoretical results will be discussed in Secs. IV C and IV D.

A. Measurement of the oscillation pressure threshold

The experimental setup described in Sec. III A is able to produce self-sustained oscillations. First, an internal pressure Pc is imposed. The initial aperture, h_0, in absence of upstream pressure, is measured by means of the optical setup. Next, the upstream pressure is continuously increased until self-sustained oscillations of the replica appear. Oscillations are quantitatively detected by a spectrum analysis as detailed in Ruty *et al.* (2005). The threshold pressure is denoted Ponset. The frequency of the oscillation at this threshold is determined by means of a spectrum analysis performed on the acoustic pressure signal. The subglottal pressure is then de-

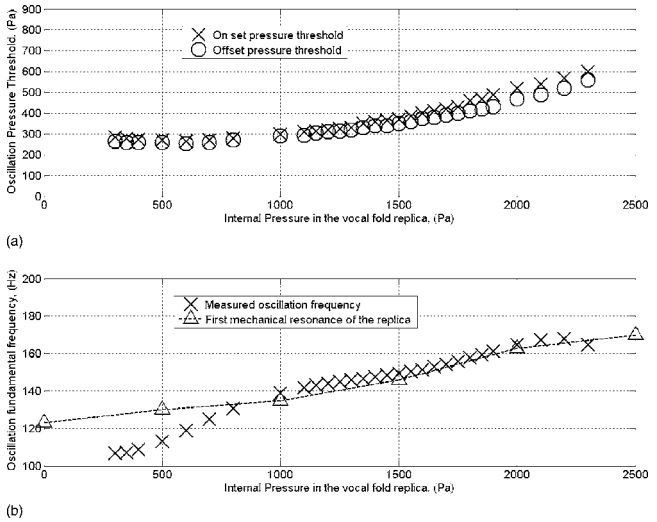

FIG. 9. Measured oscillation pressure thresholds and fundamental frequencies for a downstream resonator of 250 mm length. (a) Pressure thresholds, on-set pressure (X), off-set ($\bigcirc$). (b) Fundamental frequencies of the oscillations (X), first mechanical resonance of the replica (-△-).

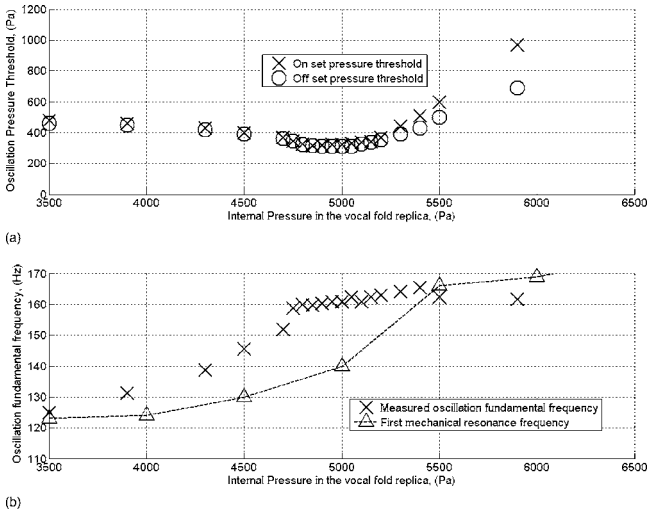

FIG. 10. Measured oscillation pressure thresholds and fundamental frequencies for a downstream resonator of 500 mm length. (a) Pressure thresholds, on-set pressure (X), off-set ($\bigcirc$). (b) Fundamental frequencies of the oscillations (X), first mechanical resonance of the replica (-△-).

creased until the oscillations cease and the associated pressure threshold, Poff-set, is recorded. This operation is repeated for several values of the internal pressure Pc, varying between 500 and 6500 Pa. The results obtained for both downstream resonators are depicted in Figs. 9 and 10.

An interesting observation is that, depending on the downstream resonator length, oscillations appear at comparable thresholds but for different internal pressure Pc. Thus, for the short resonator (250 mm), oscillations appear for low Pc values ($Pc \in [250;2500]$Pa), corresponding to a large initial aperture. For the long resonator (500 mm), oscillations appear for higher values of Pc ($Pc \in [3500;6500]$Pa). In this case, an interesting behavior is observed. An internal pressure Pc of 5000 Pa corresponds to a minimum Pon-set. At this point, the initial aperture is close to zero, i.e., the two latex tubes of the replica are almost in contact. This minimum pressure threshold, also observed by Titze *et al.* (1995), could be related to the optimal configuration to produce voiced sound, as described by Lucero (1998). Finally, in both cases, a hysteresis phenomenon, i.e., Pon-set > Poff-set, as the one described by Lucero (1999), is experimentally observed.

B. Stability analysis of the theoretical equations

In this section, we will examine if the theoretical models described in Sec. II are able to explain the experimental data. Therefore a stability analysis is applied to the proposed theoretical models.

All the variables in the theoretical equations are linearized and hence considered as the sum of an equilibrium value and a fluctuation around this equilibrium, which is denoted as $A=\bar{A}+a$ where $\bar{A}$ is the equilibrium value and a is the fluctuation. Assuming a constant subglottal pressure and a zero downstream pressure P_{supra} at the equilibrium, the following relations are obtained,

$$H_1(t) = \bar{H}_1 + h(t)_1, \quad H_2(t) = \bar{H}_2 + h_2(t), \tag{13}$$

$$P_{\text{sub}} = \bar{P}_{\text{sub}}, \quad P_{\text{supra}} = p \tag{14}$$

$$U_g = \bar{U}_g + u, \quad with\ u = \frac{\partial U_g}{\partial H_1}h_1 + \frac{\partial U_g}{\partial H_2}h_2 + \frac{\partial U_g}{\partial P_{\text{supra}}}p \tag{15}$$

$$F_i(P_{\text{sub}},P_{\text{supra}},H_1,H_2) = F_i(\bar{P}_{\text{sub}},0,\bar{H}_1,\bar{H}_2) + f_i,$$

$$with\ f_i = \frac{\partial F_i}{\partial P_{\text{supra}}}p + \frac{\partial F_i}{\partial H_1}h_1 + \frac{\partial F_i}{\partial H_2}h_2\ i = 1,2. \tag{16}$$

Considering only the fluctuating part, Eqs. (7) and (8) are rewritten as follows:

$$\frac{\partial^2 h_1(t)}{\partial t^2} = -\frac{2k}{m}h_1(t) - \frac{2k_c}{m}(h_1(t) - h_2(t)) - \frac{2r}{m}\frac{\partial h_1(t)}{\partial t} + \frac{4}{m}\left(\frac{\partial F_1}{\partial P_{\text{supra}}}p + \frac{\partial F_1}{\partial H_1}h_1 + \frac{\partial F_1}{\partial H_2}h_2\right),$$

$$\frac{\partial^2 h_2(t)}{\partial t^2} = -\frac{2k}{m}h_2(t) - \frac{2k_c}{m}(h_2(t) - h_1(t)) - \frac{2r}{m}\frac{\partial h_2(t)}{\partial t} + \frac{4}{m}\left(\frac{\partial F_2}{\partial P_{\text{supra}}}p + \frac{\partial F_2}{\partial H_1}h_1 + \frac{\partial F_2}{\partial H_2}h_2\right), \tag{17}$$

$$\frac{\partial^2 \psi(t)}{\partial t^2} + \frac{\omega_A}{Q_A}\frac{\partial \psi(t)}{\partial t} + \omega_A^2\psi(t) = \frac{Z_A\omega_A}{Q_A}\left(\frac{\partial U_g}{\partial H_1}h_1 + \frac{\partial U_g}{\partial H_2}h_2 + \frac{\partial U_g}{\partial P_{\text{supra}}}p\right). \tag{18}$$

Using a state-space representation with

$$x = \left[h_1\ h_2\ \psi\ \frac{\partial h_1}{\partial t}\ \frac{\partial h_2}{\partial t}\ \frac{\partial \psi}{\partial t}\right],$$

we obtained $\partial x/\partial t = Mx$ with M the state-space matrix,

$$M = \begin{bmatrix} 0 & 0 & 0 & 1 & 0 & 0 \\ 0 & 0 & 0 & 0 & 1 & 0 \\ 0 & 0 & 0 & 0 & 0 & 1 \\ -\frac{2}{m}\left(k + k_c - 2\frac{\partial F_1}{\partial H_1}\right) & \frac{2}{m}\left(k_c + 2\frac{\partial F_1}{\partial H_2}\right) & 0 & -\frac{2r}{m} & 0 & \frac{4}{m}\frac{\partial F_1}{\partial P_{\text{supra}}} \\ \frac{2}{m}\left(k_c + 2\frac{\partial F_2}{\partial H_1}\right) & -\frac{2}{m}\left(k + k_c - 2\frac{\partial F_2}{\partial H_2}\right) & 0 & 0 & -\frac{2r}{m} & \frac{4}{m}\frac{\partial F_2}{\partial P_{\text{supra}}} \\ \frac{Z_A\omega_A}{Q_A}\frac{\partial U_g}{\partial H_1} & \frac{Z_A\omega_A}{Q_A}\frac{\partial U_g}{\partial H_2} & -\omega_A^2 & 0 & 0 & -\frac{\omega_A}{Q_A} + \frac{Z_A\omega_A}{Q_A}\frac{\partial U_g}{\partial P_{\text{supra}}} \end{bmatrix}. \quad (19)$$

Assuming the simplifications made in Eq. (8), the state space vector x reduces to

$$x = \left[h_1 \ \psi \ \frac{\partial h_1}{\partial t} \ \frac{\partial \psi}{\partial t} \right].$$

Assuming $t_0 \ll 2\pi/\omega_0$, and using the Taylor-Young formula, one obtains $H_2(t) = H_1(t - t_0) = H_1(t) - t_0 \partial H_1(t)/\partial t$ and the state space matrix M becomes

$$M = \begin{bmatrix} 0 & 0 & 1 & 0 \\ 0 & 0 & 0 & 1 \\ -\frac{2}{m}\left(k - 2\frac{\partial F_1}{\partial H_1} - 2\frac{\partial F_1}{\partial H_2}\right) & 0 & -\frac{2r}{m} - t_0\frac{4}{m}\frac{\partial F_1}{\partial H_2} & \frac{4}{m}\frac{\partial F_1}{\partial P_{\text{supra}}} \\ \frac{Z_A\omega_A}{Q_A}\left(\frac{\partial U_g}{\partial H_1} + \frac{\partial U_g}{\partial H_2}\right) & -\omega_A^2 & -t_0\frac{Z_A\omega_A}{Q_A}\frac{\partial U_g}{\partial H_2} & -\frac{\omega_A}{Q_A} + \frac{Z_A\omega_A}{Q_A}\frac{\partial U_g}{\partial P_{\text{supra}}} \end{bmatrix}. \quad (20)$$

Studying the eigenvalues of M, one is able to determine the presence or absence of oscillations. More precisely, an unstable equilibrium results in an eigenvalue with a positive real part, i.e., the model parameters (spring stiffness, damping, subglottal pressure, initial geometry) correspond with oscillation. The oscillation frequency is calculated as

$$f = \text{Im}(\lambda)/(2\pi) \quad (21)$$

with λ the considered eigenvalue.

During the experimental protocol, the imposed internal pressure Pc in the vocal fold replica affects both the initial geometry as well as the mechanical properties. Next, for a given Pc, the presence of vocal fold oscillations depends on upstream pressure variations. In a similar way, for a given set of model parameters (spring stiffness, damping, subglottal pressure, initial geometry), the stability analysis is assessed for subglottal pressure values P_{sub} varying between 0 and 1000 Pa. An exemplary result of the stability analysis is illustrated in Fig. 11. For this particular case, oscillations are predicted to appear for a subglottal pressure of 485 Pa. The fundamental frequency of the oscillations is 117 Hz.

This computation is repeated for the set of all model parameters identified experimentally by means of the method described in Sec. III B. For each of the two downstream resonator models, respectively of lengths 250 and 500 mm, and for each set of control parameters (associated with an internal pressure Pc), the onset pressure threshold, Pon-set, is calculated. The pressure threshold and fundamental frequencies obtained for the two models of vocal folds are compared with the experimental results, as depicted in Figs. 12 and 13.

C. Discussion

The results predicted with the theoretical models, for the two downstream resonators, show their capacity to reproduce qualitatively what happens experimentally, in terms of oscillation threshold pressure and fundamental frequency, but within a large error range.

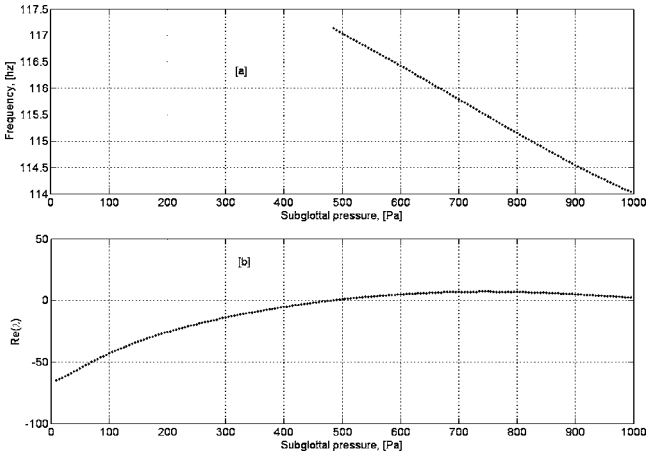

FIG. 11. Graphs resulting from the stability analysis. (a) Frequency of the oscillations, if they exist. (b) Eigenvalue real part.

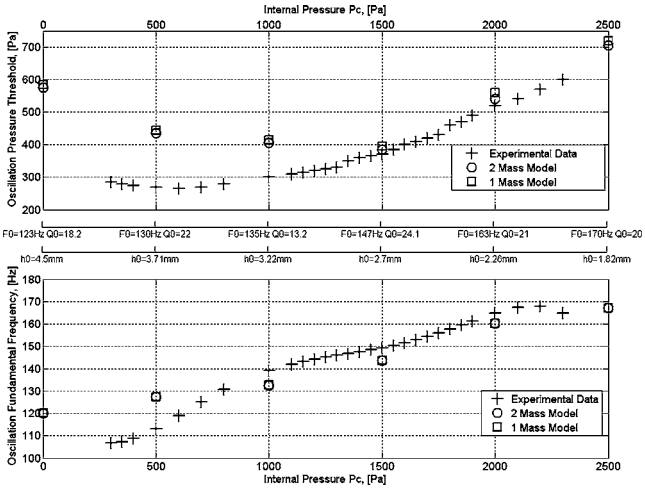

FIG. 12. Comparative study of the stability analysis result for the two theoretical models and the experimental results, for a 250 mm length downstream resonator. (a) Oscillation pressure threshold for experimental data (+), two-mass model (○), and one-mass model (□). (b) Fundamental frequency of the oscillations for experimental data (+), two-mass model (○), and one-mass model (□).

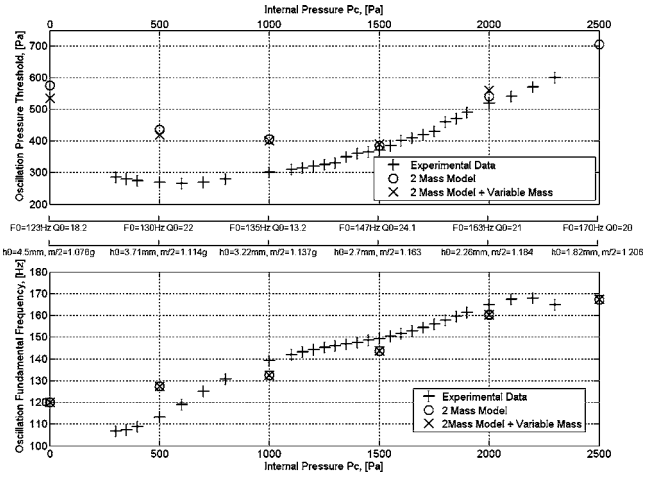

FIG. 14. Comparative study of the stability analysis result for the two-mass model with the two different mass estimations and the experimental results, for a 250 mm length downstream resonator. (a) Oscillation pressure threshold for experimental data (+), two-mass model (○), and two-mass model with a variable mass (X). (b) Fundamental frequency of the oscillations for experimental data (+), two-mass model (○), and two-mass model with a variable mass (X).

More precisely, concerning the fundamental frequency, a good accuracy of all theoretical models can be noted (agreement within 10%). As expected, the fundamental frequency increases when the internal pressure Pc is increased since increasing the internal pressure also increases the tension of the latex replica. This effect is well predicted in the theoretical models since an increase of the internal pressure in the experimental setup is associated with an increase of the spring stiffness in the theoretical models.

Concerning the oscillation threshold, the same order of magnitude and the same global behaviors are obtained. Globally, the same U-shaped behavior of the pressure threshold as a function of the internal pressure, Pc, is predicted by all theoretical models except when the vocal folds are in contact at rest position ($h_0=0$). In such a case, large departures from

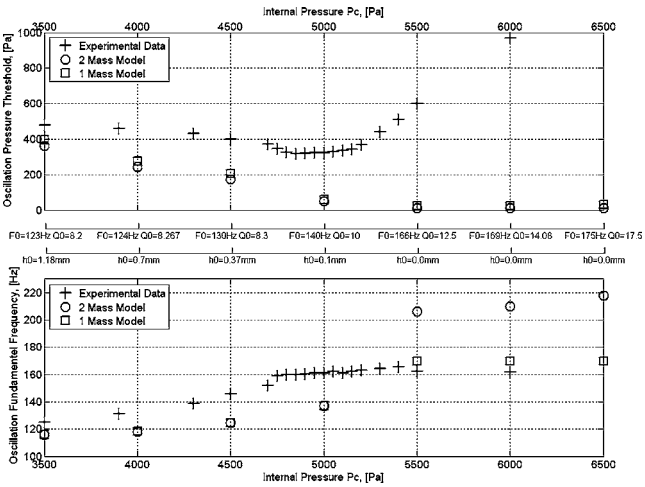

FIG. 13. Comparative study of the stability analysis result for the two theoretical models and the experimental results, for a 500 mm length downstream resonator. (a) Oscillation pressure threshold for experimental data (+), two-mass model (○), and one-mass model (□). (b) Fundamental frequency of the oscillations for experimental data (+), two-mass model (○), and one-mass model (□).

the theoretical predictions can be observed. When the vocal fold are not in contact at rest ($Pc<5500$ Pa), the delayed mass and two-mass models tend to provide comparable estimations for both the oscillation threshold pressure and fundamental frequency.

Quantitatively, although better for the longer acoustical resonator, the agreement between the predicted pressure thresholds and the measured data is rather poor except near the minimum threshold. Note that the value of the delay, t_0, does not change quantitatively the adequacy of the delayed model. These departures can, of course, be due to the theoretical models themselves but, also, to some extent, to a bad estimation of some input parameters. For example, the total mass, m, is estimated in a geometrical way as described in Sec. III B. This estimation assumes that the mass, m, is independent of the internal pressure, Pc, which is not true in the case of the latex replica. Indeed, for low internal pressures Pc, the latex tubes contain less water than for high values of Pc, where the latex tubes are inflated. To account for this effect, an alternative is to adjust the mass estimation by taking into account the geometrical and hence mass variations due to imposing different internal pressures. Considering an approximation of the latex tube deformation, depicted in Fig. 5(b), the estimation of the mass is modified as follows,

$$m = \rho_e L \frac{\pi(d_l + (h_{\text{ref}} - h_0)/4)^2}{8}, \tag{21'}$$

where h_{ref} is a reference aperture of 3 mm, and h_0 is the measured initial aperture of the replica for a given internal pressure Pc, which can be seen in Fig. 8.

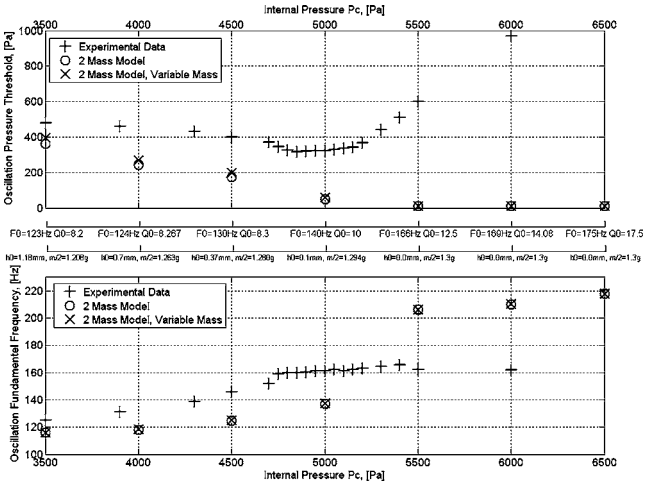

FIG. 15. Comparative study of the stability analysis result for the two-mass model with the two different mass estimations and the experimental results, for a 500 mm length downstream resonator. (a) Oscillation pressure threshold for experimental data (+), two-mass model (○), and two-mass model with a variable mass (X). (b) Fundamental frequency of the oscillations for experimental data (+), two-mass model (○), and two-mass model with a variable mass (X).

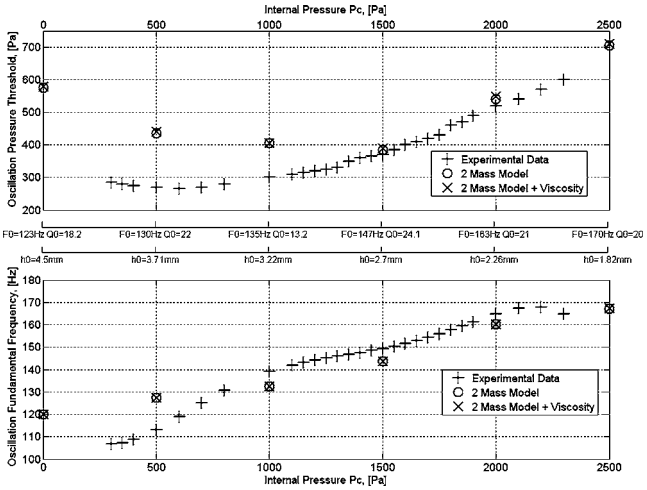

FIG. 16. Comparative study of the stability analysis result for the two mass model with additional viscosity and experimental data, for a 250 mm length downstream resonator. (a) Oscillation pressure threshold for experimental data (+), two-mass model (○), and two-mass model+viscous flow model (X). (b) Fundamental frequency of the oscillations for experimental data (+), two-mass model (○), and two-mass model+viscous flow model (X).

After this correction, the predicted oscillation thresholds are altered within an order of magnitude of 10% as shown on Figs. 14 and 15. If $h_0 > h_{\text{ref}}$, the oscillation threshold is decreased, while if $h_0 < h_{\text{ref}}$, the oscillation threshold is increased. The choice of this parameter does not seem to explain the departures observed between the measured data and the theoretical predictions.

Next the influence of the flow model is considered by taking into account viscosity in the flow model. Adding a Poiseuille term, Eqs. (1) and (2) become

$$P_{\text{sub}} - P(x,t) = \frac{1}{2}\rho U_g^2\left(\frac{1}{A^2(x,t)}\right) - 12\mu L_g^2 U_g \int_{x_0}^{x} \frac{dx}{A^3(x,t)}, \quad \text{if } x < x,$$

$$P(x,t) = P_{\text{supra}}, \quad \text{if } x > x, \tag{22}$$

where μ indicates the viscosity coefficient of the air and

$$U_g = \frac{12\mu L_g^2 \int_{x_0}^{x_s} [dx/A^3(x,t)] + \sqrt{(12\mu L_g^2 \int_{x_0}^{x_s} [dx/A^3(x,t)])^2 + 2(P_{\text{sub}} - P_{\text{supra}})\rho(1/A_s^2)}}{\rho(1/A_s^2)}. \tag{23}$$

The resulting simulations including the suggested modifications are depicted in Figs. 16 and 17. For large initial aperture no striking differences between the two flow descriptions can be found. As expected, the differences are significant in the case of small apertures corresponding to partial or complete closure of the glottis. At these points, the accounting for viscosity increases the accuracy in terms of prediction the pressure thresholds, in particular when the vocal folds are almost in contact, as well as in terms of fundamental frequency prediction. Indeed, at these points, the viscous term becomes dominant because of $1/A^3(x,t)$. However, the proposed corrections seem to not be completely sufficient to explain the quantitative differences observed between theoretical predictions and experimental data, which remain of the order of magnitude of 20%.

V. CONCLUSION

An experimental setup suitable to validate theoretical models of flow-structure-acoustic interaction with applications to voiced sound production is presented. The approach is illustrated on reduced low-order models for which the quantitative relationship between required model parameters, like mass and spring constants, and the physical characteristics of the replica can be fully exploited and controlled in order to validate the models.

Comparison between the low-order model predictions and experimental data can be summarized as follows:

(i) Despite their simplicity, the theoretical model outcomes are found to be qualitatively correct in terms of fundamental frequency and pressure threshold evolution as a function of the internal pressure of the rep-

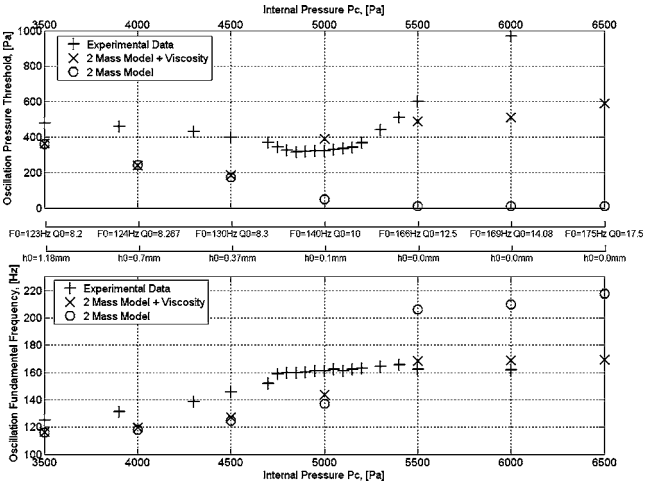

FIG. 17. Comparative study of the stability analysis result for the two-mass model with additional viscosity and the experimental data, for a 500 mm length downstream resonator. (a) Oscillation pressure threshold for experimental data (+), two-mass model (○), and two-mass model+viscous flow model (X). (b) Fundamental frequency of the oscillations for experimental data (+), and two-mass model (○), two-mass model+viscous flow model (X).

lica when the vocal folds are not in contact. In this later case, taking into account viscosity seems necessary.

(ii) The influence of the acoustical coupling is qualitatively well predicted by the theoretical models.

(iii) Viscosity of air appears to be crucial when very small glottal apertures (up to closed glottis) are involved and prediction of the oscillation pressure threshold is aimed.

(iv) While the fundamental frequency of the self-sustained oscillations is well predicted, the error ranges with respect to quantitative prediction of the oscillation pressure threshold is still large. Although an improved model outcome could be yielded by adjusting the model parameters, it is argued that the inaccuracies are mainly due to the nature of the validated reduced models themselves. Accounting for three-dimensional motions of the folds or for a better flow description during the initiation of the oscillation are examples of obvious weaknesses of the described one- and two-mass models.

(v) Lastly, the experimentally observed hysteresis has not been analyzed in the theoretical models, although several studies show that reduced order models are able to predict the observed hysteresis between on and off-set pressure necessary to sustain the oscillations. This was the case for a two-mass model analyzed by Lucero and Koenig (2005), and also for a one-mass model with a delay factor presented in two papers by Lucero (2005, 1999).

ACKNOWLEDGMENTS

This research was partially supported by a Ph.D. Grant from the French Ministry of Research and Education and by the French/German project Popaart (CNRS-MAE). We would like to acknowledge Pierre Chardon for his help building the mechanical setup, and Freek van Uittert for his help designing the data acquisition chain.

Alipour, F., and Scherer, R. C. (**2001**). "Effects of oscillation of mechanical hemi-larynx model on mean transglottal pressures and flows," J. Acoust. Soc. Am. **110**, 1562–1569.

Avanzini, F., Alku, P., and Karjalainen, M. (**2001**). "One-delayed-mass Model for Efficient Synthesis of Glottal Flow," Proc. Eurospeech Conf., Aalborg, pp. 51–54.

Baken, R. J. (**1987**). *Clinical Measurement of Speech and Voice* (Allyn and Bacon),

Barney, A., Shadle, C. H., and Davies, P. O. A. L. (**1999**). "Fluid flow in a dynamic mechanical model of the vocal folds and tract. I. Measurements and theory," J. Acoust. Soc. Am. **105**, 444–455.

Berry, D. A., and Titze, I. R. (**1996**). "Normal modes in a continuum model of vocal fold tissues," J. Acoust. Soc. Am. **100**, 3345–3354.

Berry, D. A., Herzel, H., Titze, I. R., and Krischer, K. (**1994**). "Interpretation of biomechanical simulations of normal and chaotic vocal fold oscillation with empirical eigenfunctions," J. Acoust. Soc. Am. **95**, 3595–3604.

Chan, R. W., Titze, I. R., and Titze, M. R. (**1997**). "Further studies of phonation threshold pressure in a physical model of vocal fold mucosa," J. Acoust. Soc. Am. **101**, 3722–3727.

Childers, D. G., and Wong, C.-F. (**1994**). "Measuring and modeling vocal source-tract interaction," IEEE Trans. Biomed. Eng. **41**, 663–671.

Cranen, B. (**1987**). "*The Acoustic Impedance of the Glottis. Measurement and Modelling*" (Sneldruk Enschede, The Netherlands).

Cullen, J. S., Gilbert, J., and Campbell, D. M. (**2000**). "Brass instruments: linear stability analysis and experiments with an artificial mouth," Acta Acust. **86**, 704–24.

Deverge, M., Pelorson, X., Vilain, C., Lagrée, P.-Y., Chentouf, F., Willems, J., and Hirschberg, A. (**2003**). "Influence of the collision on the flow through *in vitro* rigid models of the vocal folds," J. Acoust. Soc. Am. **114**, 3354–3362.

De Vries, M. P., Schutte, H. K., and Verkerke, G. J. (**1999**). "Determination of parameters for lumped parameter models of the vocal folds using a finite-element approach," J. Acoust. Soc. Am. **106**, 3620–3628.

Drioli, C. (**2005**). "A flow waveform-matched low-dimensional glottal model based on physical knowledge," J. Acoust. Soc. Am. **117**, 3184–3195.

Fitch, J. L., and Holbrook, A. (**1970**). "Model fundamental frequency of young adults," Arch. Otolaryngol. **92**, 379–382.

Flanagan, J. L. (**1972**). "Voices of men and machines," J. Acoust. Soc. Am. **51**, 1375–1387.

Flanagan, J. L., and Landgraf, L. (**1968**). "Self-oscillating source for vocal tract synthesizers," IEEE Trans. Audio Electroacoust. **AU-16**, 57–64.

Flanagan, J. L., Ishizaka, K., and Shipley, K. L. (**1975**). "Synthesis of speech from a dynamic model of the vocal cords and vocal tract," Bell Syst. Tech. J. **54**, 485–506.

Gauffin, J., and Liljencrants, J. (**1988**). "Modeling the Air Flow in the Glottis," Ann. Bull. RILP **22**, 41–52.

Gauffin, J., Binh, N., Ananthapadmanabha, T. V., and Fant, G. (**1983**). "Glottal geometry and volume velocity waveform," in *Vocal Fold Physiology: Contemporary Research and Clinical Issues*, edited by D. Bless and J. Abbs (College-Hill, San Diego CA), pp. 194–201.

Gilbert, J., Ponthus, S., and Petiot, J. F. (**1998**). "Artificial buzzing lips and brass instruments: experimental results," J. Acoust. Soc. Am. **104**, 1627–1632.

Herzel, H., Berry, D., Titze, I., and Saleh, M. (**1994**). "Analysis of vocal disorders with methods from non linear dynamics," J. Speech Hear. Res. **37**, 1008–1019.

Hirano, M., Kurita, S., and Nakashima, T. (**1983**). "Growth, development and aging of human vocal folds," in *Vocal Fold Physiology: Contemporary Research and Clinical Issues*, edited by D. M. Bless and J. M. Abbs, (College-Hill, San Diego, CA), pp. 22–43.

Hofmans, G. C. J., Groot, G., Ranucci, M., Graziani, G., and Hirschberg, A. (**2003**). "Unsteady flow through *in vitro* models of the glottis," J. Acoust. Soc. Am. **113**, 1658–1675.

Hollien, H., and Moore, P. (**1960**). "Measurements of the vocal folds during changes in pitch," J. Speech Hear. Res. **3**, 157–165.

Hunter, E. J., Titze, I. R., and Alipour, F. (**2004**). "A three-dimensional model of vocal fold abduction/adduction," J. Acoust. Soc. Am. **115**, 1747–1757.

Ishizaka, K., and Flanagan, J. L. (**1972**). "Synthesis of Voiced Sounds From a Two-Mass Model of the Vocal Cords," Bell Syst. Tech. J. **51**, 1233–1267.

Kaneko, T., Komatsu, K., Suzuki, H., Kanesaka, T., Masuda, T., Numata, T., and Naito, J. (**1983**). "Mechanical properties of the human vocal fold-Resonance characteristics in living humans and in excised larynges," in *Vocal Fold Physiology: Biomechanics, Acoustics and Phonatory Control*, edited by I. R. Titze and R. C. Scherer (Denver Center for the Performing Arts, Denver, CO), pp. 304–317.

Kiritani, S., Imagawa, H., Imaizumi, S., and Saito, S. (**1987**). "Measurement of air flow pattern through a mechanically driven oscillating slit: a preliminary report," Ann. Bull. RILP **21**, 1–8.

Kob, M. (**2002**). "Physical modeling of the singing voice," Ph.D. thesis, Logos-Verl, Berlin.

Lous, N. J. C., Hofmans, G. C. J., Veldhuis, N. J., and Hirschberg, A. (**1998**). "A symetrical two-mass model vocal-fold model coupled to vocal tract and trachea, with application to prothesis design," Acustica **84**, 1135–1150.

Lucero, J. C. (**2005**). "Bifurcations and limit cycles in a model for a vocal fold oscillator," Commun. Math. Sci. **3**, 517–529.

Lucero, J. C. (**1999**). "A theoretical study of the hysteresis phenomenon at vocal fold oscillation onset-offset," J. Acoust. Soc. Am. **105**, 423–431.

Lucero, J. C. (**1998**). "Optimal glottal configuration for ease of phonation," J. Voice **12**, 151–158.

Lucero, J. C. and Koenig, L. L. (**2005**). "Phonation thresholds as a function of laryngeal size in a two-mass model of the vocal folds," J. Acoust. Soc. Am. **118**, 2798–2801.

Mantha, S., Mongeau, L., and Siegmund, T. (**2005**). "Dynamic digital image correlation of a dynamic physical model of the vocal folds," 4th International Workshop MAVEBA 2005, pp. 125–128.

Mc Glone, R. E. and Shipp, T. (**1971**). "Some physiological correlates of vocal fry phonation," J. Speech Hear. Res. **14**, 769–775.

Pelorson, X., Hirschberg, A., Wijnands, A. P. J., and Baillet, H. (**1995**). "Description of the flow through in-vitro models of the glottis during phonation," Acta Acust. **3**, 191–202.

Pelorson, X., Hirschberg, A., Van Hassel, R. R., Wijnands, A. P.J., and Auregan, Y. (**1994**). "Theoretical and experimental study of quasisteady-flow separation within the glottis during the phonation. Application to a modified two-mass model," J. Acoust. Soc. Am. **96**, 3416–3431.

Pierce, A. D. (**1991**). *Acoustics: An Introduction to its Physical Principles and Applications*, 1989 ed. (Acoustical Society of America, Melville, NY).

Rothenberg, M. (**1980**). "Acoustic interaction between the glottal source and the vocal tract," in *Vocal Fold Physiology*, edited by K. N. Stevens and M. Hirano (Univ. of Tokyo, Tokyo), pp. 305–328.

Ruty, N., Van Hirtum, A., Pelorson, X., Lopez, I., and Hirschberg, A. (**2005**). "A mechanical experimental setup to simulate vocal folds vibrations. Preliminary results," ZAS papers in Linguistics, pp. 162–175⟨http://www.zas.gwz-berlin.de/papers/zaspil/articles/zp40/ruty_final2.pdf⟩.

Saito, S., Fukuda, K., Suzuki, H., Komatsu, K., Kanesaka, T., and Kobayashi, N. (**1981**). "X-ray stroboscopy," in *Vocal Fold Physiology*, edited by K. N. Stevens and M. Hirano (Univ. of Tokyo, Tokyo), pp. 95–106.

Scherer, R. C. and Guo, R. C. (**1990**). "Effect of vocal fold radii in pressure distributions in the glottis," J. Acoust. Soc. Am. **88** (Suppl. 1), S150.

Scherer, R. C., Titze, I. R., and Curtis, J. F. (**1983**). "Pressure-flow relationships in two models of the larynx having rectangular glottal shapes," J. Acoust. Soc. Am. **73**, 668–676.

Scherer, R. C., Shinwari, D., De Witt, K. J., Zhang, C., Kucinschi, B. R., and Afjeh, A. A. (**2001**). "Intraglottal pressure profiles for a symmetric and oblique glottis with a divergence angle of 10 degrees," J. Acoust. Soc. Am. **109**, 1616–1630.

Story, B. H. and Titze, I. R. (**1995**). "Voice simulation with body cover model of the vocal folds," J. Acoust. Soc. Am. **97**, 1249–1260.

Svec, J. G., Horacek, J., Sram, F., and Vesely, J. (**2000**). "Resonance properties of the vocal folds: *In vivo* laryngoscopic investigation of the externally excited laryngeal vibrations," J. Acoust. Soc. Am. **108**, 1397–1407.

Thomson, S. L., Mongeau, L., and Frankel, S. H. (**2005**). "Aerodynamic transfer to the vocal folds," J. Acoust. Soc. Am. **118**, 1689–1700.

Titze, I. R. (**1988**). "The physics of small-amplitude oscillation of the vocal folds," J. Acoust. Soc. Am. **83**, 1536–1552.

Titze, I. R., Schmidt, S. S., and Titze, M. R. (**1995**). "Phonation threshold pressure in a physical model of the vocal fold mucosa," J. Acoust. Soc. Am. **97**, 3080–3084.

Vampola, T., Horáček, J., Veselý, J., Vokřál ∃ (**2005**). "Modelling of influence of velopharyngeal insufficiency on phonation of vowel /a/," 4th International Workshop MAVEBA 2005, pp. 43–46.

Van den Berg, Jw., Zantema, J. T., and Doornenbal, P. (**1957**). "On the air resistance and the Bernoulli effect of the human larynx," J. Acoust. Soc. Am. **29**, 625–631.

Vilain, C. E., Pelorson, X., Hirschberg, A., Le Marrec, L., Op't Root, W., and Willems, J. (**2003**). "Contribution to the physical modeling of the lips. Influence of the mechanical boundary conditions," Acta. Acust. Acust. **89**, 882–887.

Wong, D., Ito, M. R., Cox, N. B., and Titze, I. R. (**1991**). "Observation of perturbations in a lumped-element model of the vocal folds with application to some pathological cases," J. Acoust. Soc. Am. **89**, 383–394.